Title

Water Table Dynamics and Biogeochemical Cycling in a Shallow, Variably-Saturated Floodplain

Journal

Environmental Science and Technology, 51(6)

ISSN

0013-936X

Authors

Yabusaki, Steven B

Wilkins, Michael J

Fang, Yilin

et al.

Publication Date

2017-03-21

DOI

10.1021/acs.est.6b04873

Peer reviewed

Environmental Science & Technology

Article

pubs.acs.org/est

Water Table Dynamics and Biogeochemical Cycling in a Shallow, Variably-Saturated Floodplain

Steven B. Yabusaki,*[,†] Michael J. Wilkins,[‡] Yilin Fang,[†] Kenneth H. Williams,[§] Bhavna Arora,[§] John Bargar,[∥] Harry R. Beller,[§] Nicholas J. Bouskill,[§] Eoin L. Brodie,[§] John N. Christensen,[§] Mark E. Conrad,[§] Robert E. Danczak,[‡] Eric King,[§] Mohamad R. Soltanian,[‡] Nicolas F. Spycher,[§] Carl I. Steefel,[§] Tetsu K. Tokunaga,[§] Roelof Versteeg,[⊥] Scott R. Waichler,[†] and Haruko M. Wainwright[§]

[†]Pacific Northwest National Laboratory, Richland, Washington 99354, United States

[‡]The Ohio State University, Columbus, Ohio 43210, United States

[§]Lawrence Berkeley National Laboratory, Berkeley, California 94720, United States

[∥]Stanford Synchrotron Radiation Lightsource, SLAC National Accelerator Laboratory, Menlo Park, California 94025, United States

[⊥]Subsurface Insights, Hanover, New Hampshire 03755, United States

Supporting Information

ABSTRACT: Three-dimensional variably saturated flow and multicomponent biogeochemical reactive transport modeling, based on published and newly generated data, is used to better understand the interplay of hydrology, geochemistry, and biology controlling the cycling of carbon, nitrogen, oxygen, iron, sulfur, and uranium in a shallow floodplain. In this system, aerobic respiration generally maintains anoxic groundwater below an oxic vadose zone until seasonal snowmelt-driven water table peaking transports dissolved oxygen (DO) and nitrate from the vadose zone into the alluvial aquifer. The response to this perturbation is localized due to distinct physico-biogeochemical environments and relatively long time scales for transport through the floodplain aquifer and vadose zone. Naturally reduced zones (NRZs) containing sediments higher in organic matter, iron sulfides, and non-crystalline U(IV) rapidly consume DO and nitrate to maintain anoxic conditions, yielding Fe(II) from FeS oxidative dissolution, nitrite from denitrification, and U(VI) from nitrite-promoted U(IV) oxidation. Redox cycling is a key factor for sustaining the observed aquifer behaviors despite continuous oxygen influx and the annual hydrologically induced oxidation event. Depth-dependent activity of fermenters, aerobes, nitrate reducers, sulfate reducers, and chemolithoautotrophs (e.g., oxidizing Fe(II), S compounds, and ammonium) is linked to the presence of DO, which has higher concentrations near the water table.

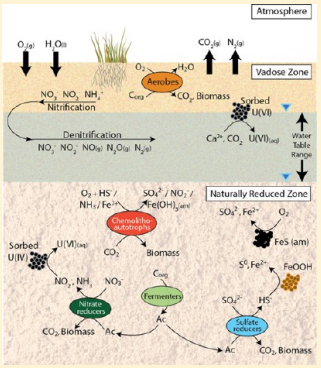

INTRODUCTION

The biogeochemical response of floodplain ecosystems to changes in hydrologic forcing will be an important component of long-term adaptive management strategies.[1] These systems of coupled processes contribute to the modulation of terrestrial carbon and nitrogen fluxes[2] but also control the mobility of metals.[3] Seasonal hydrologic variability leads to dynamic flow and reactive transport through local subsurface biogeochemical environments, which influence microbial structure and function.[4] Redox cycling, mediated by local geochemical and microbial reactivity, is important to the 1) mobility of metals (e.g., iron, manganese, uranium, vanadium, selenium, arsenic); 2) maintenance of floodplain carbon and nitrogen exchange with the atmosphere; and 3) replenishment of reductive capacity depleted by oxidation during seasonal hydrologic events. The interplay of coupled hydrology, geochemistry, and biology in a river-aquifer-vadose zone system under changing conditions is thus central to the development of a systematic understanding and basis for predictive models of floodplain functioning and services.

In this study, we use three-dimensional (3D) variably saturated flow and biogeochemical reactive transport modeling to build a systematic and mechanistic understanding of the processes, properties, and conditions controlling spatially and temporally variable biogeochemistry in a small, semiarid floodplain of the Colorado River in western Colorado that was once the site of a uranium mill. The shallow alluvial aquifer at the Old Rifle site has been the subject of interdisciplinary research conducted by the U.S. Department of Energy (DOE), beginning in 2002[5] with a focus on *in situ* uranium bioremediation primarily in the context of small-scale (~15 m) field experiments.[6−8]

Recently, the breadth and scale of the research at the Rifle site was expanded to examine the hydrobiogeochemistry of the entire floodplain,[9−12] which is bounded to the south by a ~ 750

Received: September 26, 2016
Revised: February 15, 2017
Accepted: February 20, 2017
Published: February 20, 2017

DOI: 10.1021/acs.est.6b04873
Environ. Sci. Technol. 2017, 51, 3307−3317

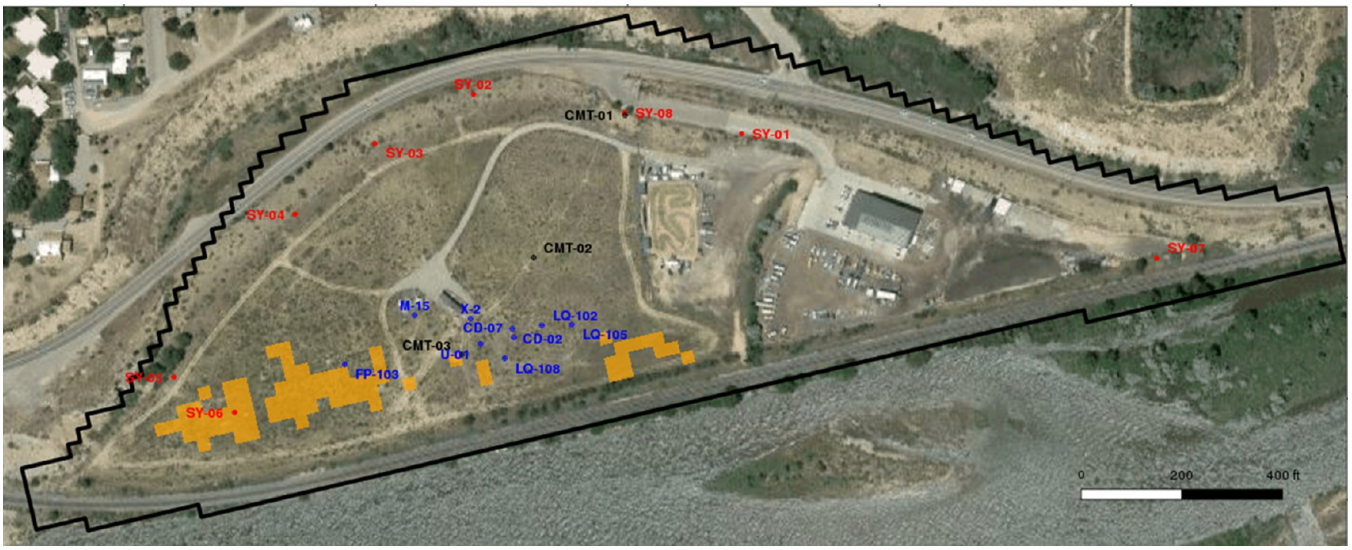

Figure 1. Rifle floodplain with modeling domain boundaries (black line), naturally reduced zones (orange), and well locations. Well label colors: biogeochemical wells (black), boundary wells (red), and monitoring wells (blue).

m shoreline with the Colorado River and to the north by a crescent-shaped outcrop of the relatively impermeable Wasatch formation, which is ~250 m from the river at its widest point (Figure 1). The Wasatch formation also underlies the floodplain, providing a bottom confining contact ~20 ft (~6 m) below ground surface for the shallow floodplain aquifer. During base flow conditions, the saturated thickness above the Wasatch contact is mostly in a range of 7 to 12 ft (2.1 to 3.7 m).

In the subsurface of the Rifle floodplain, near-atmospheric levels of oxygen gas are always present above the water table in unsaturated pores, free to dissolve into the porewater, and subsequently diffuse and disperse into the saturated zone. Dissolved oxygen (DO) levels (up to 2 mg/L) can generally be found in the first few centimeters of groundwater just below the water table. Below this layer for most of the year, groundwater is generally anoxic (<0.5 mg/L DO, > 0.1 mg/L Fe^{2+}), indicating that oxygen consumption rates in the aquifer are sufficiently high to suppress DO concentrations.

A seasonal, snowmelt-driven water table rise beginning in April typically peaks 3 to 5 ft (0.9 to 1.5 m) higher in June, before receding to pre-snowmelt levels in August. During water table peaking, the background reducing capacity of the aquifer can be temporarily overwhelmed. The biogeochemical response to the water table peaking event is spatially and temporally variable. Some locations are able to maintain low redox potentials throughout the water table peaking event.[10] The maintenance of these conditions requires relatively rapid and sustained oxidant-consuming reactions. Locations where this behavior has been observed appear to be correlated with "naturally reduced zones" (NRZs) enriched with organic matter, sulfides and reduced metals.[11,13] The NRZs are "hot spots"[14−17] that provide an opportunity to better understand the interplay between the seasonal hydrologic forcing; mixing of vadose zone DO and nitrate into groundwater; abiotic redox and mineral geochemistry; and microbiological processes that are aerobic and anaerobic, oxidizing and reducing, and encompass heterotrophic, chemolithoautotrophic, and fermentative metabolisms. The reaction rates and redox cycling revealed during the water table peaking event can yield important general insights on the fluxes of carbon, oxygen, nitrogen, and metals in the floodplain aquifer and vadose zone.

Challenges to understanding redox behaviors in the Rifle floodplain include 1) limiting reactants that are rapidly consumed and therefore, not directly measured, and 2) relatively large, seemingly unchanging concentrations that mask smaller but important changes in the system. Thus, it is difficult to determine fluxes and/or reaction rates for oxygen, nitrate, sulfate, and carbon from geochemical observations alone. In the absence of definitive geochemical confirmation for the processes of interest, "omics" analyses (e.g., proteogenomics) and/or isotopic fractionation may provide the only proxy evidence for some reactions, rates, and fluxes of interest.

RECENT STUDIES

The shallow vadose zone is a source for oxygen, nitrate and carbon that is transported to the groundwater. NRZs, delineated by borehole lithology, biogeochemical sampling, and time domain induced polarization,[11,13] are seen to have an important role in the spatially and temporally variable responses to the water table peaking event. Rapid oxygen depletion in NRZ sediments has been experimentally determined to be dominated by the abiotic oxidative dissolution of iron sulfide minerals to Fe(II) and sulfate.[10] The iron sulfide minerals form from the reaction of Fe(II) with sulfide generated via the activity of sulfate-reducing bacteria (SRB).[18] Micromolar Fe(II) concentrations are generally present in the groundwater, with the highest concentrations found in the NRZs. During the water table peaking event, dissolved Fe(II) in the studied NRZ increases by a factor of 2 or more.

The persistence of ~1 μM uranium in the groundwater has been linked to the oxidation state and form of uranium, as well as the principal oxidants in the floodplain, oxygen, and nitrate.[19,20] During the water table peaking event, U(VI) levels in the NRZ increase 40 to 50%. This is consistent with the oxidation of a U(IV) phase[20−22] that is solubilized when exposed to an effective oxidant.[18,23] This U(IV) has been characterized to be dominantly monomeric as opposed to crystalline (e.g., uraninite) form.[20,22]

DOI: 10.1021/acs.est.6b04873
Environ. Sci. Technol. 2017, 51, 3307−3317

A variety of genomic, transcriptomic, and proteomic data have been collected from wells across the floodplain.[10,24−28] This has informed a general classification of metabolic function including fermentation, aerobic respiration, sulfate reduction, nitrate and nitrite reduction, iron oxidation, sulfur and sulfide oxidation, and anammox (anaerobic ammonia oxidation). In particular, proteomics-inferred metabolisms include oxygen- and nitrate-dependent Fe(II) oxidation (*Gallionellaceae*), fermentation of organic matter (OD1, OP11, and *Clostridiaceae*), nitrate reduction (multiple microorganisms), and microaerophilic heterotrophy (*Comamonadaceae and Rhodocyclaceae*).[24,28] Putative methanogenic sequences were less than 0.1% relative abundance in the 16S rRNA gene analysis[10] and a higher-resolution analysis did not recover methanogen genomes in metagenomic data sets.[28] Archaea were present at low relative abundances (generally between 1 and 3% relative abundance based on 16S rRNA gene data). A prior study at the Rifle site that focused exclusively on archaeal genomes recovered from groundwater indicated that these groups were primarily performing organic carbon fermentation.[29]

Fermenters and sulfate reducers are generally considered to be obligate anaerobes, but some species appear to increase in abundance during the oxygenation induced by the water table peaking event:[10] 16S rRNA gene analyses indicate that putative fermenters affiliated with the Parcubacteria (OD1-L1) are most abundant during the most oxygenated conditions in the background aquifer, with higher abundances at deeper depths where DO is lower. Conversely, in the generally anoxic NRZ, sequences matching OD1-L1 are typically more abundant in the shallowest groundwater samples where DO is low but higher than at depth. This potentially implies tolerance of more microaerophilic conditions, a trend that has also been observed in oxic sediments at the Hanford site.[30]

Previous field experiments[5−8] at the site have demonstrated that indigenous metal- and sulfate-reducing heterotrophs are carbon-limited and can be stimulated and enriched by amending groundwater with acetate, a lower molecular weight electron donor with a relatively high nominal oxidation state of carbon (NOSC[31]) of zero. Both metagenomics and 16S rRNA[10] gene analyses indicate that the most abundant SRB in the Rifle subsurface are members of *Desulfobulbaceae, Desulfobacteraceae, and Desulfuromonadaceae*. These groups are generally classified as anaerobes that are strongly inhibited by the elevated oxygen during the water table peaking event. The highest relative abundances are found in the NRZs, with increasing relative abundance with depth (i.e., further from the highest oxygen concentrations).

Metatranscriptomic analyses of the Rifle subsurface have provided evidence for non-heterotrophic oxidation pathways via chemolithoautotrophs.[32] These organisms can couple the oxidation of chemical species such as Fe(II), reduced S compounds, and ammonium to the reduction of oxygen, nitrate, and nitrite while fixing carbon for biomass. These biologically mediated processes are contributing to the maintenance of anoxic aquifer conditions.

Many species of bacteria responsible for heterotrophic aerobic respiration also have the ability to reduce nitrate. Members of the *Comamonadaceae* and *Rhodocyclaceae* are two examples. Microorganisms within these families are generally considered to be facultative anaerobes, and are relatively abundant during the oxygenation of the background aquifer, generally increasing in abundance as DO enters the aquifer. In the studied NRZ, in which anoxic conditions are generally maintained over most of the vertical profile, shifts in the relative abundance of inferred aerobic microorganisms were only observed in the shallowest samples during the oxygenation event.[10]

A recent modeling analysis of the Rifle floodplain[9] demonstrated that abiotic reactions alone could not account for the vertical distribution of observed CO_2 gas concentrations in the vadose zone. This CO_2 distribution is consistent with a biological source near the top of the capillary fringe with upward, gradient-driven diffusion to the ground surface. Organic carbon is elevated in the sediments nearest to the water table,[13] which is consistent with a heterotrophic process inferred to be dominated by aerobic respiration, as oxygen is the most abundant terminal electron acceptor and provides the largest energy yield for a microbially mediated terminal electron accepting process (TEAP).

METHODS

The Rifle floodplain hydrogeology, sampling methodology, and analytical methods have largely been described elsewhere.[7,10,12,33] In this study, the uranium concentrations in wells SY-02 and SY-08 were determined through samples collected from tubing placed 15 ft (4.6 m) below ground surface in the fully screened wells, with quantitation via Kinetic Phosphorescence Analyzer (KPA). In the multilevel TT/CMT (vadose zone/aquifer) wells, ammonium concentrations were measured colorimetrically via the reduction of sodium salicylate; nitrate and nitrite concentrations were measured via ion chromatography using Thermo Fisher Scientific's ICS-2100 ion chromatograph equipped with an AS-18 analytical column. Vadose zone oxygen gas concentrations were measured with a 2014 Shimadzu gas chromatograph.

MODEL SPECIFICATION

This study targets the 2014 Rifle floodplain water table peaking event based on hydrobiogeochemical observations. A pair of previous modeling studies focused on the biogeochemical impacts of a seasonal water table peaking event in three tandem multilevel vadose zone-groundwater wells aligned with the predominant flow direction in the Rifle floodplain aquifer.[10,14] The present study expands on the previous work by explicitly addressing vadose zone measurements and processes as well as the dynamics of flow and reactive transport across the entire floodplain. Nitrogen and uranium biogeochemistry has been incorporated into the modeling to address observed behaviors including uranium dynamics in two perimeter wells. The reaction network for the functional guilds in this study has been updated with rate law parameterizations that better account for oxygen sensitivity. The intent is to use a floodplain-wide modeling framework to better understand and interpret the interplay of processes, properties, and conditions leading to the observed behaviors. The modeling is informed by previous and ongoing Rifle studies, continuously monitored water levels across the floodplain, and a small number of tandem vadose zone−groundwater sampling locations where water chemistry and 16S rRNA gene sequences were collected and analyzed. Detailed biogeochemistry for this event was collected at three locations, one of which was in an NRZ. While this small number of biogeochemical sampling locations limits the modeling to a scoping level of analysis for the floodplain, the modeling framework does provide context for these local processes through the systematic integration of information

DOI: 10.1021/acs.est.6b04873
Environ. Sci. Technol. 2017, 51, 3307−3317

from surface geophysics, lithologic and mineralogical studies, and the monitoring of water levels and water quality parameters in other wells. We also acknowledge limitations associated with the use of 16S rRNA gene surveys as the microbial foundation for this modeling effort, including potential amplification biases and the inability of these primers to detect some recently detected members of the bacterial tree of life due to the presence of multiple insertions with the 16S rRNA gene sequences.[25] However, the data analysis performed in Danczak et al. (2016) demonstrated that the primers used in this study did detect a significant fraction of members of the candidate phyla radiation (CPR) in Rifle groundwater. As always, designing universal primers that target newly detected phyla is an ongoing challenge.

The eSTOMP[34] three-dimensional (3D) variably saturated flow (i.e., Richards Equation) and multicomponent biogeochemical reactive transport code was used to model the Rifle floodplain. The model domain resolves boundary geometry and spatial property distributions using 104 940 grid cells with 7.6 m lateral resolution and 0.3 m vertical resolution. The 1 year simulation used a nominal time step of 6 h (adaptive refinement can internally reduce the time step size to improve the solution convergence and efficiency), primarily to resolve the water level dynamics in the river and aquifer. Massively parallel processing was necessary to address the high-performance computing and large memory requirements for modeling the coupled hydrologic, abiotic, and biotic processes controlling the observed dynamic redox behaviors involving carbon, nitrogen, oxygen, iron, sulfur, and uranium.

Variably saturated flow in the Rifle floodplain subsurface for 2014 is driven by transient water level measurements along the upgradient aquifer boundary and river shore, and a constant, uniform 3 cm/year net surface recharge.[12] The subsurface is represented by two lithofacies: (1) a sandy gravel comprising the alluvial aquifer and the vadose zone, and (2) a weathered bedrock claystone (Wasatch Formation) that provides bottom and lateral confinement for the alluvial aquifer.[9] The vertical and lateral extent of the lithofacies distributions is based on borehole lithologic logs and electrical resistivity tomography geophysics.[11] Hydrogeologic properties and saturation function parameters for the lithofacies are based on previous studies[9,35] and listed in Table SI-1. The NRZs comprise centimeter-scale features of limited lateral extent (<2 m),[22] that are considerably smaller than the grid resolution (0.3 m vertically, 7.6 m laterally). The model represents the NRZs as geochemical, not physical, heterogeneities. Dispersivities for DO and nitrate were increased by a factor of 10 from previous studies (nominal values in Table SI-1) to reflect the enhanced vertical mixing observed throughout the floodplain aquifer. The vertical mixing efficiency during water table peaking is a unique feature of the Rifle floodplain that cannot be reproduced with transport parameters from previous Rifle modeling of field experiments. Notably, these experiments were all performed after the seasonal water table peaking event with amendment release from fully screened wells.

The initial spatial distribution of reactive phases in this study is based on sediment characterizations performed at a limited number of locations in the Rifle floodplain.[10,13,22] The distribution of organic matter is related to the floodplain depositional history. Higher particulate organic carbon (POC) abundance near the bottom of the vadose zone is consistent with elevated CO_2 production there. Measured dissolved organic carbon (DOC) ca. 0.3 mM in the aquifer (Figure SI-1) may reflect less-bioavailable, higher-molecular-weight organic matter, as these levels do not appear to be correlated with seasonal biological activity or CO_2 gas production. The abundance and oxidation states of Fe, S, and U phases, as well as the distribution of solid-phase organic C have been statistically correlated with the NRZs.[13] In particular, FeS is in higher abundance at depth in the NRZs.[10,13,22] Non-invasive surface-based time-domain induced polarization geophysics was used along with borehole lithological logs to delineate the NRZs in 3D in the floodplain aquifer.[11] The NRZs are estimated to comprise <3% of the floodplain aquifer volume (H. Wainwright, personal communication).

Aqueous initial and boundary conditions are based on observed chemistry.[9] Carbon and nitrogen cycling begins with the breakdown of organic matter via an aerobic respiration process yielding organic carbon that is more bioavailable and ammonium. The model uses cellulose to represent the residue mix comprising organic matter. Nitrification of ammonium and nitrite via obligate aerobic autotrophic reactions is assumed to produce the vadose zone nitrate. Significant insight into DO and nitrate entering the NRZs was provided by observations in the background aquifer, where limited reactivity led to increasing concentrations of these species during water table peaking. In the more-reactive NRZ sediments, DO and nitrate were essentially absent, nitrite was present, and biological nitrate reduction was confirmed through omics and $^{15}N/^{18}O$-NO_3 isotopic fractionation. To account for the DO and nitrate entering the aquifer during the water table peaking event, we used observations in the background aquifer to calibrate a time-dependent source that was uniformly distributed across the floodplain.

U(IV) is specified in the NRZs as a surface-complexed, non-crystalline phase[20,36] with concentrations consistent with previous Rifle studies.[22] We model U(IV) as a surface-complexed monomeric species.[36] In the NRZs, FeS mineral contributes to the maintenance of anoxic conditions that generally protect U(IV) from oxidation and mobilization.[37] U(IV) can potentially be oxidized abiotically by DO, nitrate, denitrification intermediates, and Fe(III), and by direct (e.g., *Thiobacillus denitrificans*[38,39]) and indirect (via Fe(III) from nitrate-dependent Fe(II) oxidation) biotic U(IV) oxidation.[39] For the conditions in the NRZ during water table peaking (i.e., increasing Fe(II) and nitrite), nitrite is the most likely U(IV) oxidant.[22,40] In the model specification, surface-complexed, non-crystalline U(IV)[36] is abiotically oxidized by nitrite to U(VI) and mobilized. This is consistent with previous U(IV) oxidation studies with Rifle sediments,[40] recent metatranscriptomic and proteogenomic inferences of extensive nitrogen cycling (including nitrate reduction) in Rifle groundwater[28,32] and nitrite observations in the studied NRZ well during the oxygenation event.

Outside of the NRZs, uranium in the floodplain aquifer is specified as aqueous and surface-complexed U(VI), consistent with observed aqueous concentrations and a three-site U(VI) surface complexation model previously developed for the Rifle sediments.[18,41] Near the northernmost point of the floodplain, U(VI) is specified in variably saturated sediments at an elevation [5305 ft (1617 m)] that is accessed during water table peaking, with concentrations consistent with observations in a nearby well.

Fe(II) is generated in the model via oxygen-promoted oxidative FeS dissolution and sulfide-promoted reductive goethite dissolution. Heterotrophic iron reduction, which has

DOI: 10.1021/acs.est.6b04873
Environ. Sci. Technol. 2017, 51, 3307−3317

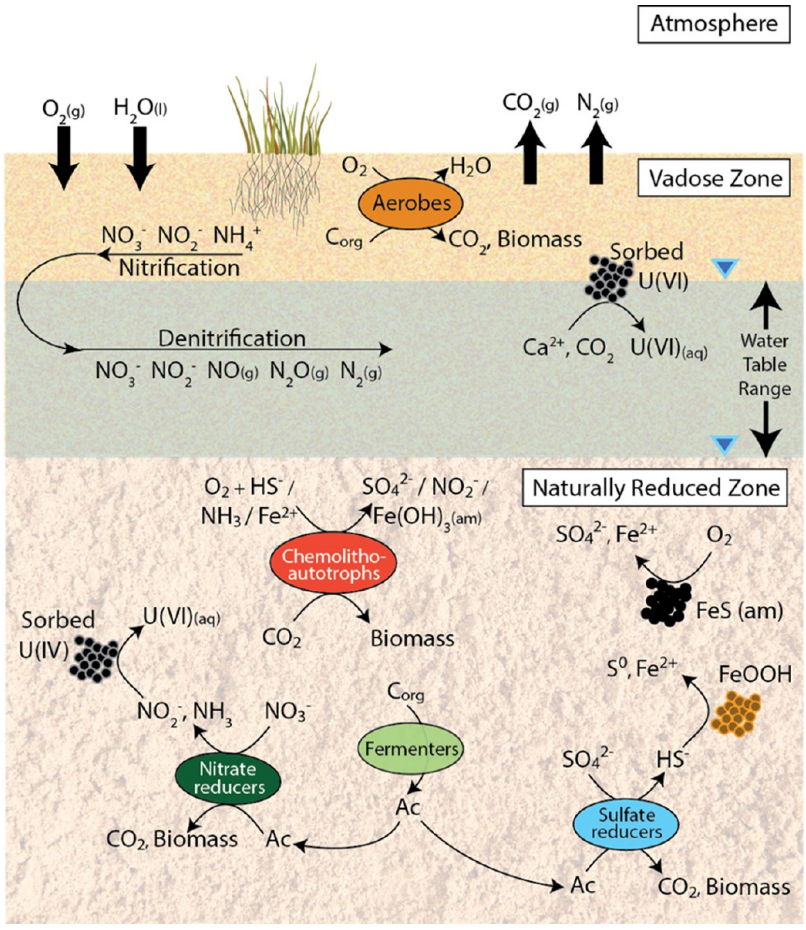

Figure 2. Schematic diagram of biogeochemistry in the naturally reduced zone, variably saturated zone, and vadose zone.

been stimulated with acetate amendment in previous Rifle studies,[5,6,8,42] is not considered significant, based on metagenomic and 16S rRNA gene analyses. Fe(II) oxidation is considered to be dominantly abiotic.[10] Other major ion geochemical reactions are based on a previous reaction network developed for Rifle groundwater.[43]

Heterotrophic aerobic respiration addresses the reduction of oxygen and the principal biogenic CO_2 production. Fermentation is included to address carbon cycling, where refractory organic matter is converted to bioavailable acetate, which is utilized by the heterotrophic oxygen, nitrate, nitrite, and sulfate TEAPs. In this case, direct enzymatic reduction of sulfate and nitrate/nitrite is supported by 16S rRNA gene and metagenomic analyses of microbial assemblages. The implication is that bioavailable organic matter in the groundwater is utilized soon after it is produced.

Redox cycling is a key feature of the processes controlling carbon, nitrogen, oxygen, iron, sulfur, and uranium behavior in the aquifer. The continuous supply of oxidants (i.e., oxygen and nitrate) to a largely anoxic aquifer with elevated alkalinity (~10 mequiv/L) favor chemolithoautotrophy. In this case, the oxidation of sulfide, Fe(II), and ammonium is coupled to the reduction of oxygen and nitrate as CO_2 is being fixed. Without replenishment, the continuous and seasonal biotic and abiotic oxidation mechanisms would eventually deplete reduced phases such as FeS. The resupply of reduced phases, supported by anaerobic heterotrophic TEAPs (e.g., sulfate reduction), is thus an important component in the long term maintenance of low redox potential in the Rifle floodplain aquifer.

Biomass generation and decay are included in the reaction network specification.[43] In the absence of detailed biomass measurements, the modeled biomass provides a relative measure of time-integrated functional activity. Inhibition terms in the Monod type rate laws are used to control activity under suboptimal conditions (e.g., obligate anaerobes under oxic conditions).[9] The model employs oxygen inhibition terms in the rate laws that reflect considerable DO tolerance by SRB, fermenters, and chemolithoautotrophs.

The biogeochemical reaction network (Tables SI-2 and SI-3) is an amalgam of previous reaction networks,[6,9,43] updated for this application. The reaction network is applied throughout the model domain with behaviors differentiated by local abundance or concentration. Figure 2 is a schematic summary of the proposed biogeochemistry in the NRZ and overlying vadose zone.

RESULTS

Observed Biogeochemical Trends in the Rifle Subsurface. In the vadose zone, ammonium concentrations are usually less than 15 μM, often below detection. However, elevated ammonium concentrations (~30−100 μM) have been measured just above the water table [10−12 ft (3.0−3.7 m) below ground surface]. Ammonium is subject to nitrification to nitrite and nitrate before denitrification to gas-phase intermediates (NO and N_2O) and, ultimately, molecular nitrogen (N_2). Nitrate concentrations in the vadose zone can be high (~5 mM, primarily in the deeper samples). In the background aquifer, nitrite is very low (~1 μM), nitrate is

DOI: 10.1021/acs.est.6b04873
Environ. Sci. Technol. 2017, 51, 3307−3317

generally less than 80 μM, and ammonium is ~25 μM but spatially variable. Conversely, in the NRZ, nitrate is generally below detection, nitrite is 80−100 μM, and ammonium is temporally and spatially variable ranging from undetectable to 80 μM. Prior to seasonal water table peaking, DO and nitrate concentrations are generally very low in the aquifer relative to the vadose zone (Figure 3). The DOC is relatively low and unchanging with time and depth in the aquifer, whereas concentrations in the vadose zone are higher with more temporal variability (Figure SI-1).

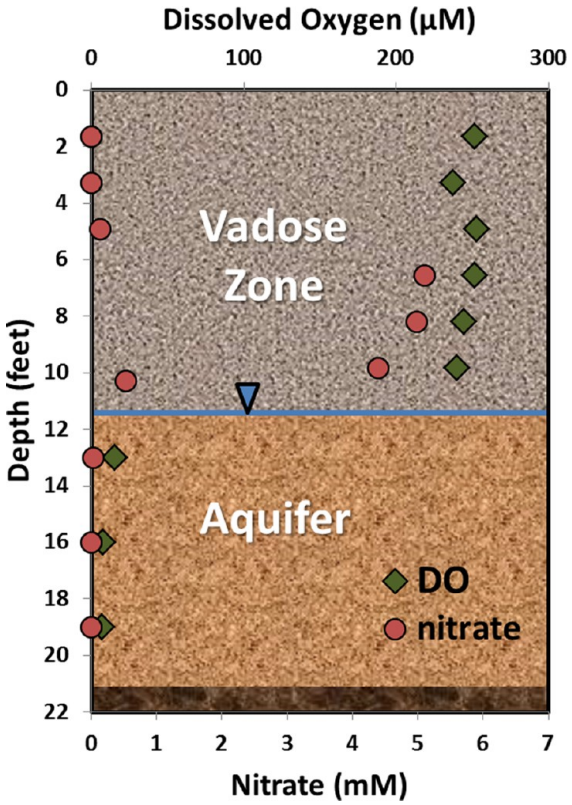

Figure 3. Depth-dependent concentrations of oxygen and nitrate in March and April of 2014 (CMT-03/TT-03). The water table on April 11, 2014 at a depth of 11.42 feet and the top of the Wasatch bottom-confining zone at a depth of 21.2 feet are shown.

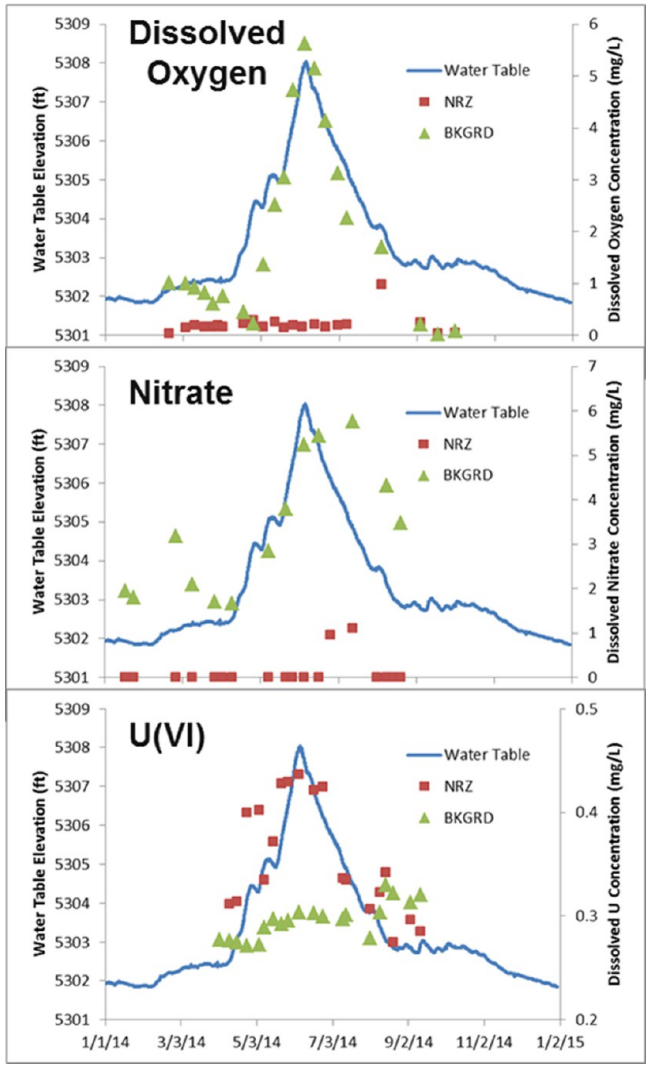

Figure 4. Water table elevation (well X-2), dissolved oxygen (top), nitrate (middle), and uranium (bottom) concentrations in background aquifer (CMT-02, green triangles) and naturally reduced zone (CMT-03, red squares). Concentrations measured in the deep sampling port (depth ≈ 19 feet).

During the water table rise and fall in 2014, DO and nitrate in the previously unsaturated vadose zone are mixed into the groundwater, resulting in elevated DO and nitrate concentrations as high as 6 mg/L at depth in the least reactive sediments. The extent of oxidant delivery to the aquifer depends on the duration and magnitude of the water table peaking event, which lasted 2 weeks in 2013 and more than 3 months in 2014.

For much of the alluvial aquifer, the elevated DO and nitrate concentrations are temporarily well-mixed to depth. Elevated aqueous Fe(II) and U(VI) are observed in the NRZ (well CMT-03 in Figure 1) during the water table peaking event.[10] Figure 4 contrasts the impact of the water table peaking event in the NRZ with the more oxidized background (well CMT-02) for DO, nitrate, and U(VI) in the groundwater. Outside of the NRZs, U(VI) concentrations (~1 μM) are generally stable. A recently discovered exception is the observation of a quickly dissipating spike in uranium concentrations (~3 μM) that occurs near the northernmost part of the floodplain when the water table rises more than 2 ft (0.6 m) above the base flow elevation of 5305 ft (1617 m). This behavior has been linked to unremediated sediments from historical milling operations that underlie the highway adjacent to the site (Figure 1). A similar phenomenon has previously been observed in a floodplain of the Columbia River on the Hanford Site.[44] These short-term U(VI) dynamics in a location with relatively low U(VI) groundwater concentrations is in contrast to relatively stable U(VI) concentrations in other non-NRZ locations (Figure SI-2).

Simulations. The variably saturated flow (Figure SI-3) modeling reproduces the time-dependent variation of water levels and gradients at multiple locations across the floodplain for the year-long 2014 simulation (Figure SI-4). While the river stage dynamics influence floodplain water levels and gradient magnitudes, the observed south−southwest regional gradient direction is largely maintained throughout the year, with the exception of a reversal at the end of May 2014 (Figure SI-5). Cumulative flow into the aquifer during the 1 year simulation is largely through the upland boundary with less than 10% from

DOI: 10.1021/acs.est.6b04873
Environ. Sci. Technol. 2017, 51, 3307−3317

the constant 3 cm/year surface recharge (Figure SI-6). Cumulative outflow is through the river boundary. Predicted daily flow rates across aquifer boundaries reveal a dynamic influx of river water induced by river stage fluctuations primarily during the spring snowmelt (Figure SI-7). The predicted penetration of river water into the aquifer was less than 25 m laterally, which is consistent with non-decreasing specific conductivity measurements (>2300 μS/cm) in the wells nearest the river, which were over 30 m from the shoreline.

Vertical recharge-driven transport results in a ~20 year travel time from ground surface to water table. For locations away from the river, cross-floodplain groundwater travel times are a minimum of 2 years. In contrast, the water table peaking occurs over a time scale of weeks and is the principal driver for the observed biogeochemical dynamics.

A defining, but non-unique, feature of the Rifle floodplain is the ~3 m thick oxic vadose zone overlying an anoxic aquifer of similar thickness. The juxtaposition of vadose zone DO and nitrate across the water table from groundwater that is largely lacking in those components drives diffusion. DO and nitrate transported into the aquifer are utilized and consumed as terminal electron acceptors for microbial respiration, a process that generally maintains the low redox potential.

Aerobic respiration, which is the principal heterotrophic process in the model, sustainably maintains anoxic aquifer conditions for most of the year and is also consistent with CO_2 production observed near the bottom of the vadose zone. Biomass growth associated with aerobic respiration trends with 16S rRNA gene relative abundances for microbial taxa containing likely aerobes (e.g., *Comamonadaceae* and *Rhodocyclaceae*) (Figure 5).

For most of the year, the largely anoxic floodplain aquifer supports sulfide production via SRB, albeit limited by organic matter bioavailability. The distribution of modeled FeS formation is consistent with preferential formation in the NRZ with depth. During oxygenated conditions, the SRB are most inhibited at shallow depths where the oxygen concentrations are highest. This is reflected in the biomass dynamics, which trend with observed spatial and temporal variability of 16S rRNA gene relative abundances for putative SRB within the *Desulfobulbaceae, Desulfobacteraceae, and Desulfuromonadaceae* (Figure 5).

The annual snowmelt-driven water table peaking event has a profound, albeit relatively short-term, impact on the biogeochemistry of the Rifle floodplain subsurface. During water table rise, the largely anoxic groundwater displaces and mixes with the vadose zone porewater but is also subject to the entrainment, dissolution, and partitioning of oxygen to the liquid phase. The principal changes induced by this event derive from groundwater access to vadose zone oxygen and nitrate with subsequent transport and mixing to depth. The biogeochemical response is seen to be strongly regulated by the local subsurface physico-biogeochemical environments. For most of the aquifer, oxygenation associated with the water table peaking event overwhelms the oxygen consuming capacity of microbial and mineral assemblages and elevated DO (up to 6 mg/L) results. In this case, the limited lateral transport and vertically well-mixed conditions result in concentrations that are dependent on the saturated thickness; i.e., more dilution where the aquifer is deeper and vice versa (Figure 6).

In the NRZs in which FeS is abundant, DO is rapidly consumed principally by abiotic oxidative dissolution of FeS,[37] maintaining anoxic conditions that permit the Fe(II) reaction

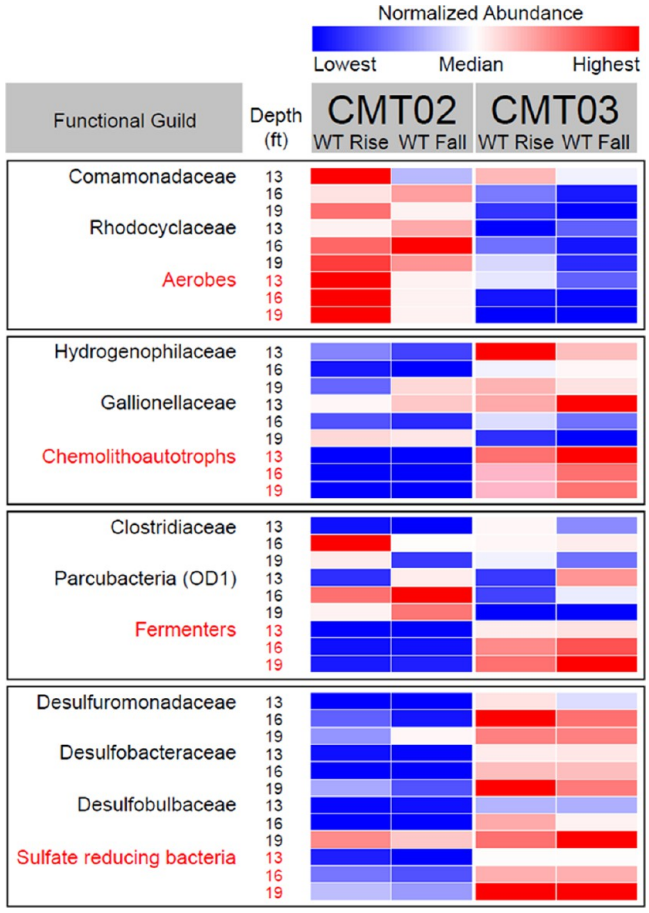

Figure 5. Heatmaps for normalized 16S rRNA gene abundances for the dominant taxa in the identified functional guilds are compared with heatmaps for normalized simulated biomass of the functional guilds to identify common trends. The comparisons address two time periods, water table rise and water table fall. Two plan view locations are shown (background aquifer (CMT-02) and NRZ (CMT-03)) and three depths (13, 16, and 19 ft). Modeled functional guilds are highlighted in red.

product to accumulate (Figure 7).[10] Sulfate, which is also a product of this reaction, is marginally increased above the 10 mM background concentrations.

The depletion of FeS in the NRZs during repeated annual oxygenation cycles is unsustainable without redox cycling. In this case, FeS is replenished as sulfide from heterotrophic sulfate reduction abiotically reacts with available Fe(II). FeS formation occurs primarily during non-oxygenated conditions, in which sulfate reduction is not inhibited.

U(IV) is principally found as an immobile phase in the NRZs, where FeS generally protects it from oxidation and mobilization during oxygenated conditions.[37] During the period of the seasonal water table rise and fall, there is a commensurate rise and fall in aqueous U(VI), which is captured by the modeling (Figure 7). While this behavior is ultimately the result of abiotic oxidation of U(IV) by nitrite, it is facilitated by nitrate entering the groundwater from the lower vadose zone, mixing to depth during the water table peaking event and heterotrophic nitrate reduction.

Elevated U(VI) in the background (i.e., non-NRZ) aquifer near the north end of the floodplain is also related to the water table peaking event but not through a redox process. In this case, the sharp increase in shallow U(VI) groundwater

DOI: 10.1021/acs.est.6b04873
Environ. Sci. Technol. 2017, 51, 3307−3317

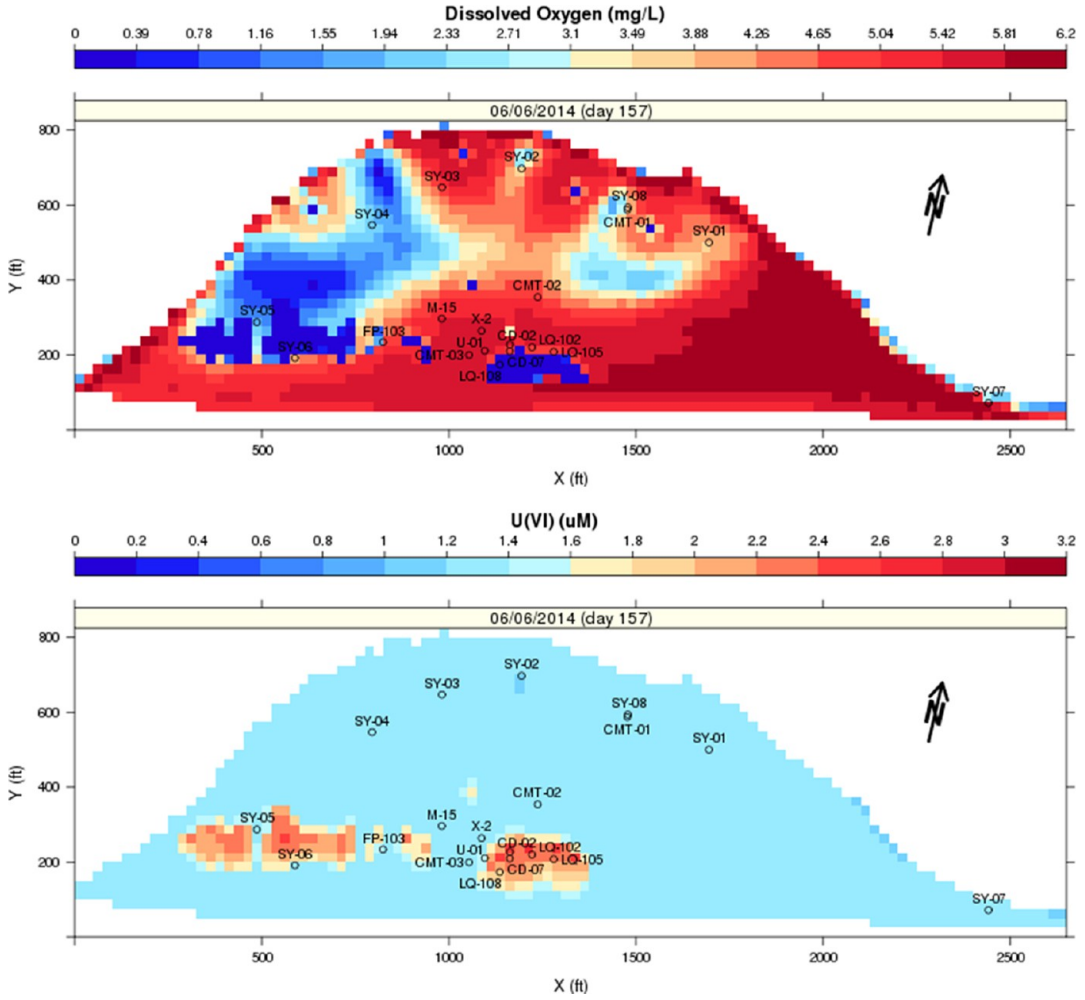

Figure 6. Simulated dissolved oxygen (top) and uranium (bottom) concentrations in the floodplain aquifer at a 5285 foot elevation on June 6, 2014.

concentrations followed by rapid dissipation (Well SY-02 in Figure SI-2) is the result of remnant U(VI) contamination in sediments that are above the water table for most of the year but are saturated and leached during the water table peaking event. This behavior is similar to that observed in column experiments with uranium-contaminated sediments in which the stoppage of flow allows buildup of uranium in the aqueous phase followed by a high concentration spike when flow is resumed.[45,46] The equilibrium uranium surface complexation model, which generally addressed the relatively stable uranium behavior in the aquifer, could not reproduce the short-term dynamics of this "perched" uranium source.

A notable feature of the Rifle floodplain aquifer is chemolithoautotrophy putatively mediating the oxidation of nitrite, ammonium, Fe(II), and sulfide. Chemolithoautotrophy is facilitated, in part, by the abundance of bicarbonate derived from heterotrophic and abiotic sources and the co-location of oxidants and reduced phases. While this situation can generally be found at the water table interface, where near-atmospheric oxygen concentrations are proximal to Fe(II) and sulfide, the annual oxygenation event significantly expands the range of depths where chemolithoautotrophy can take place, albeit temporarily. Simulated functional chemolithoautotrophic biomass shows higher activity in the NRZs during the oxygenation event, which is in agreement with 16S rRNA gene relative abundances matching members of the *Gallionellaceae* (Figure 5). A metatranscriptomic study has identified outsized activity for this Fe(II)- and S-oxidizing bacterial family during nitrate-dependent oxidation of bioreduced sediments in the Rifle floodplain.[32]

DISCUSSION

The Rifle floodplain modeling required a tight coupling of geochemical, biological, and hydrologic processes to systematically account for the observed dynamics. For most of the year, aerobic respiration can sustainably maintain anoxic conditions throughout the floodplain aquifer beneath an oxic vadose zone. However, the annual water table peaking event is a significant perturbation to the stability of the contrasting biogeochemical conditions above and below the water table. The response to this perturbation is highly localized due to distinct physico-biogeochemical environments (e.g., NRZs, vadose zone uranium) and the relatively long time scales for transport through the floodplain aquifer and the vadose zone.

The mixing of DO and nitrate from the vadose zone into the alluvial aquifer during the water table peaking event results in the rapid oxidation of reduced phases via dominantly abiotic processes. The consumption rate of oxidants in the floodplain aquifer during this time is generally insufficient to maintain anoxic conditions, which leads to elevated concentrations of DO and nitrate. In this case, the return to anoxic conditions is facilitated largely by slower biotic reactions. The exception to

DOI: 10.1021/acs.est.6b04873
Environ. Sci. Technol. 2017, 51, 3307−3317

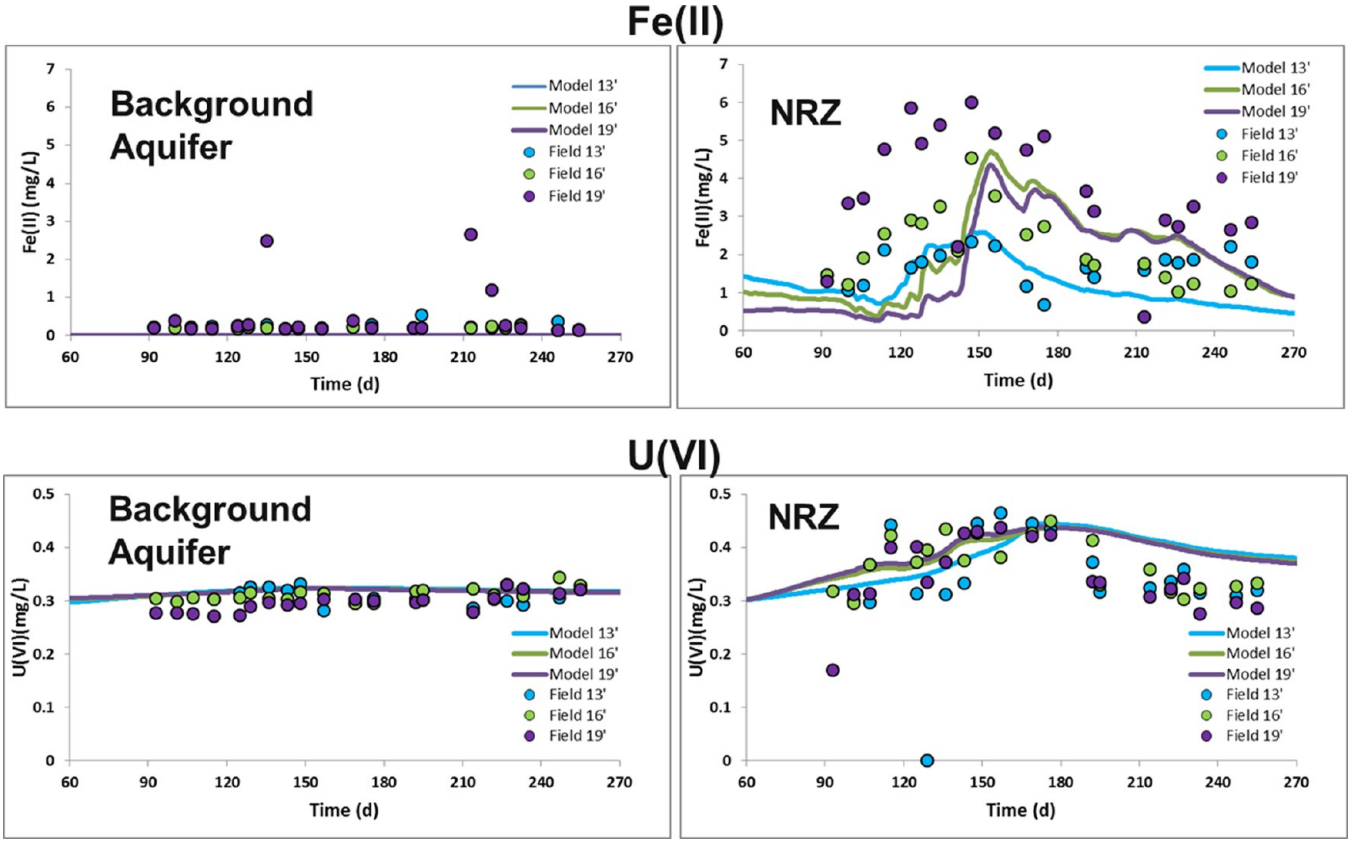

Figure 7. Time-dependent Fe(II) (top) and U(VI) (bottom) concentrations in CMT-02 (background aquifer) and CMT-03 (NRZ): modeled (lines) vs observed (dots) for 13, 16, and 19 ft depths.

this behavior occurs in NRZs, which are able to maintain anoxic conditions during water table peaking primarily due to the presence of FeS, which is sufficiently abundant to consume the supplied DO via oxidative dissolution, yielding Fe(II) and sulfate. The result is a seemingly paradoxical increase in Fe(II) during an oxygenation event. The NRZ sediments are also associated with higher organic matter content and non-crystalline U(IV). Nitrate reaching the NRZ is rapidly reduced enzymatically leading to nitrite accumulations during the water table peaking event. Under the Rifle floodplain conditions, nitrite (as well as other denitrification intermediates) is a more efficient U(IV) oxidizer than DO, which leads to elevated U(VI) concentrations in the NRZ groundwater.

Elevated U(VI) groundwater concentrations during water table peaking were also observed in a non-NRZ location. In this case, U(VI)-contaminated sediments, which reside above the water table for most of the year, are leached by groundwater during the highest water table elevations. The abiotic processes responsible for uranium mobilization during the water table peaking event are controlled, in part, by products of heterotrophic activity that increase alkalinity, which affects uranium speciation and mobility, and in the case of the NRZs, nitrite availability, which promotes U(IV) oxidation.

Sulfate concentrations in the floodplain aquifer are high (~10 mM) and relatively stable. During the water table peaking event, SRB are inhibited in the presence of elevated oxygen but are active in the NRZ. Biogenic sulfide from the reduction of sulfate catalyzed by this functional guild promotes the abiotic production of (1) Fe(II) via reductive dissolution of Fe(III) minerals (represented by goethite in the model) and (2) FeS via reaction with aqueous Fe(II). In the absence of direct enzymatic Fe(III) reduction, the former reaction appears to be the principal mechanism for Fe(II) production in the floodplain. The latter reaction is critical to the replenishment of FeS oxidized during the water table peaking event.

Chemolithoautotrophy in the Rifle floodplain aquifer is characterized by a microaerophilic lifestyle supported by the mixing of DO and nitrate into a largely anoxic aquifer with elevated alkalinity and the presence of reduced S, Fe, or N species. These conditions are found just below the water table and in the NRZs during the water table peaking event. Chemolithoautotrophs provide another mechanism for the oxidation of sulfide, Fe(II), and ammonium as CO_2 is being fixed.

In the Rifle floodplain, redox cycling of carbon, oxygen, nitrogen, iron, sulfur, and uranium is facilitated by coupled geochemistry, heterotrophy, and chemolithoautotrophy. The aggregate effect on the floodplain from the imposed conditions is a net import of O_2 and export of CO_2 and N_2. Redox cycling is a key control for sustaining these fluxes in spite of seasonal, hydrologically induced oxidation events.

Riparian floodplains are at the hydrologic intersection of inflow from upland catchments, net recharge from local precipitation and evapotranspiration, and discharge controlled by river stage. Changing hydrologic conditions are seen to influence microbial structure and metabolism in the context of local physico-biogeochemical environments. Clearly, floodplain hydrology, geochemistry, and biology are intertwined, regulating the cycling of redox-active species that control terrestrial carbon and nitrogen fluxes. This relatively short modeling time frame, based on a few intensely monitored locations, was a modest scoping step toward the goal of building a systematic

DOI: 10.1021/acs.est.6b04873
Environ. Sci. Technol. 2017, 51, 3307−3317

and mechanistic understanding of the interplay between these processes, properties, and conditions. This understanding will be needed to predict floodplain ecosystem functioning under changing hydrology. Next steps should include surface processes with plants and roots, additional "omics" analyses for greater resolution of microbial functionality, gas-phase transport measurements for the vadose zone, differentiation of bioavailable organic carbon forms (including microbial biomass), and linkage of these forms of organic carbon to organisms and rates.

■ ASSOCIATED CONTENT

Supporting Information

The Supporting Information is available free of charge on the ACS Publications website at DOI: 10.1021/acs.est.6b04873.

Figures showing dissolved organic carbon and U(VI) concentrations, saturated thickness during water table peak, a comparison of water levels, gradient direction and magnitude, cumulative flow into the floodplain aquifer, and daily flow rates. Tables showing material properties for the lithofacies, equilibrium reactions, species and formation constants, kinetic reactions, and rate constants. (PDF)

■ AUTHOR INFORMATION

Corresponding Author

*E-mail: yabusaki@pnnl.gov.

ORCID

Steven B. Yabusaki: 0000-0003-1040-0182

Tetsu K. Tokunaga: 0000-0003-0861-6128

Author Contributions

All authors have given approval to the final version of the manuscript.

Funding

This material is based upon work supported as part of the Genomes to Watershed Scientific Focus Area at Lawrence Berkeley National Laboratory funded by the U.S. Department of Energy, Office of Science, Office of Biological and Environmental Research under Award Number DE-AC02-05CH11231. A portion of the work described in this article was performed at Pacific Northwest National Laboratory, which is operated by Battelle for the United States Department of Energy under Contract DE-AC05-76RL01830. Massively parallel processing simulations were performed using the Cascade supercomputer at the Environmental Molecular Sciences Laboratory, a DOE Office of Science User Facility sponsored by the Office of Biological and Environmental Research and located at Pacific Northwest National Laboratory.

Notes

The authors declare no competing financial interest.

■ ACKNOWLEDGMENTS

Dick Dayvault was an integral part of all research performed at the Rifle Site. He managed many of the details of the drilling campaigns, data collection, field experiments, and supporting infrastructure. We will miss him but the memory of his commitment and enthusiasm for the research at Rifle will always be an inspiration.

■ ABBREVIATIONS

CPR	candidate phyla radiation
DO	dissolved oxygen
DOC	dissolved organic carbon
DOE	U.S. Department of Energy
NRZ	naturally reduced zone
POC	particulate organic carbon
SRB	sulfate-reducing bacteria
TEAP	terminal electron accepting process

■ REFERENCES

(1) Welti, N.; Bondar-Kunze, E.; Singer, G.; Tritthart, M.; Zechmeister-Boltenstern, S.; Hein, T.; Pinay, G. Large-scale controls on potential respiration and denitrification in riverine floodplains. *Ecological Engineering* **2012**, *42*, 73−84.

(2) Harms, T. K.; Grimm, N. B. Influence of the hydrologic regime on resource availability in a semi-arid stream-riparian corridor. *Ecohydrology* **2010**, *3* (3), 349−359.

(3) Schulz-Zunkel, C.; Rinklebe, J.; Bork, H.-R. Trace element release patterns from three floodplain soils under simulated oxidized−reduced cycles. *Ecological Engineering* **2015**, *83*, 485−495.

(4) Freimann, R.; Bürgmann, H.; Findlay, S. E. G.; Robinson, C. T. Hydrologic linkages drive spatial structuring of bacterial assemblages and functioning in alpine floodplains. *Front. Microbiol.* **2015**, *6*.10.3389/fmicb.2015.01221

(5) Anderson, R. T.; Vrionis, H. A.; Ortiz-Bernad, I.; Resch, C. T.; Long, P. E.; Dayvault, R.; Karp, K.; Marutzky, S.; Metzler, D. R.; Peacock, A.; White, D. C.; Lowe, M.; Lovley, D. R. Stimulating the in situ activity of Geobacter species to remove uranium from the groundwater of a uranium-contaminated aquifer. *Appl. Environ. Microbiol.* **2003**, *69* (10), 5884−5891.

(6) Long, P. E.; Williams, K. H.; Davis, J. A.; Fox, P. M.; Wilkins, M. J.; Yabusaki, S. B.; Fang, Y. L.; Waichler, S. R.; Berman, E. S. F.; Gupta, M.; Chandler, D. P.; Murray, C.; Peacock, A. D.; Giloteaux, L.; Handley, K. M.; Lovley, D. R.; Banfield, J. F. Bicarbonate impact on U(VI) bioreduction in a shallow alluvial aquifer. *Geochim. Cosmochim. Acta* **2015**, *150*, 106−124.

(7) Williams, K. H.; Long, P. E.; Davis, J. A.; Wilkins, M. J.; N'Guessan, A. L.; Steefel, C. I.; Yang, L.; Newcomer, D.; Spane, F. A.; Kerkhof, L. J.; McGuinness, L.; Dayvault, R.; Lovley, D. R. Acetate Availability and its Influence on Sustainable Bioremediation of Uranium-Contaminated Groundwater. *Geomicrobiol. J.* **2011**, *28* (5−6), 519−539.

(8) Vrionis, H. A.; Anderson, R. T.; Ortiz-Bernad, I.; O'Neill, K. R.; Resch, C. T.; Peacock, A. D.; Dayvault, R.; White, D. C.; Long, P. E.; Lovley, D. R. Microbiological and geochemical heterogeneity in an in situ uranium bioremediation field site. *Appl. Environ. Microbiol.* **2005**, *71* (10), 6308−6318.

(9) Arora, B.; Spycher, N. F.; Steefel, C. I.; Molins, S.; Bill, M.; Conrad, M. E.; Dong, W.; Faybishenko, B.; Tokunaga, T.; Wan, J.; Williams, K. H.; Yabusaki, S. B. Influence of Hydrological, Biogeochemical and Temperature Transients on Subsurface Carbon Fluxes in a Flood Plain Environment. *Biogeochemistry* **2016**, *127* (2), 367−396.

(10) Danczak, R.; Yabusaki, S.; Williams, K.; Fang, Y.; Hobson, C.; Wilkins, M. J. Snowmelt induced hydrologic perturbations drive dynamic microbiological and geochemical behaviors across a shallow riparian aquifer. *Frontiers in Earth Science* **2016**, *4*.10.3389/feart.2016.00057

(11) Wainwright, H. M.; Flores-Orozco, A.; Bucker, M.; Dafflon, B.; Hubbard, S. S.; Williams, K. H.; Chen, J. Hierarchical Bayesian method for mapping biogeochemical hot spots using induced polarization imaging. *Water Resour. Res.* **2016**, *52*, 533−551.

(12) Tokunaga, T. K.; Kim, Y.; Conrad, M. E.; Bill, M.; Hobson, C.; Williams, K. H.; Dong, W.; Wan, J.; Robbins, M. J.; Long, P. E.; Faybishenko, B.; Christensen, J. N.; Hubbard, S. S. Deep Vadose Zone Respiration Contributions to Carbon Dioxide Fluxes from a Semiarid Floodplain. *Vadose Zone J.* **2016**, *15*, (7).010.2136/vzj2016.02.0014

(13) Campbell, K. M.; Kukkadapu, R.; Qafoku, N. P.; Peacock, A. D.; Lesher, E.; Williams, K. H.; Bargar, J. R.; Wilkins, M. J.; Figueroa, L.;

Ranville, J.; Davis, J. A.; Long, P. E. Geochemical, mineralogical and microbiological characteristics of sediment from a naturally reduced zone in a uranium-contaminated aquifer. *Appl. Geochem.* **2012**, *27*, 1499−1511.
(14) Arora, B.; Dwivedi, D.; Hubbard, S. S.; Steefel, C. I.; Williams, K. H. Identifying geochemical hot moments and their controls on a contaminated river floodplain system using wavelet and entropy approaches. *Environmental Modelling & Software* **2016**, *85*, 27−41.
(15) McClain, M. E.; Boyer, E. W.; Dent, C. L.; Gergel, S. E.; Grimm, N. B.; Groffman, P. M.; Hart, S. C.; Harvey, J. W.; Johnston, C. A.; Mayorga, E.; McDowell, W. H.; Pinay, G. Biogeochemical Hot Spots and Hot Moments at the Interface of Terrestrial and Aquatic Ecosystems. *Ecosystems* **2003**, *6* (4), 301−312.
(16) Andrews, D. M.; Lin, H.; Zhu, Q.; Jin, L.; Brantley, S. L. Hot Spots and Hot Moments of Dissolved Organic Carbon Export and Soil Organic Carbon Storage in the Shale Hills Catchment. *Vadose Zone J.* **2011**, *10* (3), 943−954.
(17) Bao, C.; Wu, H.; Li, L.; Newcomer, D.; Long, P. E.; Williams, K. H. Uranium Bioreduction Rates across Scales: Biogeochemical Hot Moments and Hot Spots during a Biostimulation Experiment at Rifle, Colorado. *Environ. Sci. Technol.* **2014**, *48* (17), 10116−10127.
(18) Fang, Y.; Yabusaki, S. B.; Morrison, S. J.; Amonette, J. P.; Long, P. E. Multicomponent reactive transport modeling of uranium bioremediation field experiments. *Geochim. Cosmochim. Acta* **2009**, *73* (20), 6029−6051.
(19) Zachara, J. M.; Long, P. E.; Bargar, J.; Davis, J. A.; Fox, P.; Fredrickson, J. K.; Freshley, M. D.; Konopka, A. E.; Liu, C.; McKinley, J. P.; Rockhold, M. L.; Williams, K. H.; Yabusaki, S. B. Persistence of uranium groundwater plumes: Contrasting mechanisms at two DOE sites in the groundwater−river interaction zone. *J. Contam. Hydrol.* **2013**, *147* (0), 45−72.
(20) Bargar, J. R.; Williams, K. H.; Campbell, K. M.; Long, P. E.; Stubbs, J. E.; Suvorova, E. I.; Lezama-Pacheco, J. S.; Alessi, D. S.; Stylo, M.; Webb, S. M.; Davis, J. A.; Giammar, D. E.; Blue, L. Y.; Bernier-Latmani, R. Uranium redox transition pathways in acetate-amended sediments. *Proc. Natl. Acad. Sci. U. S. A.* **2013**, *110* (12), 4506−4511.
(21) Bone, S. E.; Dynes, J. J.; Cliff, J.; Bargar, J. R. Uranium(IV) adsorption by natural organic matter in anoxic sediments. *Proc. Natl. Acad. Sci. U. S. A.* **2017**, *114*, 711.
(22) Janot, N.; Lezama-Pacheco, J. S.; Pham, D. Q.; O'Brien, T. M.; Hausladen, D.; Noël, V.; Maher, K.; Fendorf, S.; Williams, K. H.; Long, P. E.; Bargar, J. R.; Lallier, F. Physico-chemical heterogeneity of organic-rich sediments in the Rifle aquifer, CO: Impact on uranium biogeochemistry. *Environ. Sci. Technol.* **2016**, *50* (1), 46−53.
(23) Lezama-Pacheco, J. S.; Cerrato, J. M.; Veeramani, H.; Alessi, D. S.; Suvorova, E.; Bernier-Latmani, R.; Giammar, D. E.; Long, P. E.; Williams, K. H.; Bargar, J. R. Long-Term in Situ Oxidation of Biogenic Uraninite in an Alluvial Aquifer: Impact of Dissolved Oxygen and Calcium. *Environ. Sci. Technol.* **2015**, *49* (12), 7340−7347.
(24) Wrighton, K. C.; Castelle, C. J.; Wilkins, M. J.; Hug, L. A.; Sharon, I.; Thomas, B. C.; Handley, K. M.; Mullin, S. W.; Nicora, C. D.; Singh, A.; Lipton, M. S.; Long, P. E.; Williams, K. H.; Banfield, J. F. Metabolic interdependencies between phylogenetically novel fermenters and respiratory organisms in an unconfined aquifer. *ISME J.* **2014**, *8* (7), 1452−1463.
(25) Brown, C. T.; Hug, L. A.; Thomas, B. C.; Sharon, I.; Castelle, C. J.; Singh, A.; Wilkins, M. J.; Wrighton, K. C.; Williams, K. H.; Banfield, J. F. Unusual biology across a group comprising more than 15% of domain Bacteria. *Nature* **2015**, *523* (7559), 208−211.
(26) Hug, L. A.; Thomas, B. C.; Brown, C. T.; Frischkorn, K. R.; Williams, K. H.; Tringe, S. G.; Banfield, J. F. Aquifer environment selects for microbial species cohorts in sediment and groundwater. *ISME J.* **2015**, *9* (8), 1846−1856.
(27) Castelle, C. J.; Wrighton, K. C.; Thomas, B. C.; Hug, L. A.; Brown, C. T.; Wilkins, M. J.; Frischkorn, K. R.; Tringe, S. G.; Singh, A.; Markillie, L. M.; et al. Genomic Expansion of Domain Archaea Highlights Roles for Organisms from New Phyla in Anaerobic Carbon Cycling. *Curr. Biol.* **2015**, *25* (6), 690−701.
(28) Hug, L. A.; Thomas, B. C.; Sharon, I.; Brown, C. T.; Sharma, R.; Hettich, R. L.; Wilkins, M. J.; Williams, K. H.; Singh, A.; Banfield, J. F. Critical biogeochemical functions in the subsurface are associated with bacteria from new phyla and little studied lineages. *Environ. Microbiol.* **2016**, *18* (1), 159−173.
(29) Castelle, C. J.; Wrighton, K. C.; Thomas, B. C.; Hug, L. A.; Brown, C. T.; Wilkins, M. J.; Frischkorn, K. R.; Tringe, S. G.; Singh, A.; Markillie, L. M. Genomic Expansion of Domain Archaea Highlights Roles for Organisms from New Phyla in Anaerobic Carbon Cycling. *Curr. Biol.* **2015**, *25* (6), 690−701.
(30) Nelson, W. C.; Stegen, J. C. The reduced genomes of Parcubacteria (OD1) contain signatures of a symbiotic lifestyle. *Front. Microbiol.* **2015**, *6*, 713.
(31) LaRowe, D. E.; Van Cappellen, P. Degradation of natural organic matter: A thermodynamic analysis. *Geochim. Cosmochim. Acta* **2011**, *75* (8), 2030−2042.
(32) Jewell, T. N. M.; Karaoz, U.; Brodie, E. L.; Williams, K. H.; Beller, H. R. Metatranscriptomic evidence of pervasive and diverse chemolithoautotrophy relevant to C, S, N, and Fe cycling in a shallow alluvial aquifer. *ISME J.* **2016**, *10* (9), 2106−2117.
(33) Long, P. E.; Williams, K. H.; Davis, J. A.; Fox, P. M.; Wilkins, M. J.; Yabusaki, S. B.; Fang, Y.; Waichler, S. R.; Berman, E. S. F.; Gupta, M.; Chandler, D. P.; Murray, C.; Peacock, A. D.; Giloteaux, L.; Handley, K. M.; Lovley, D. R.; Banfield, J. F. Bicarbonate impact on U(VI) bioreduction in a shallow alluvial aquifer. *Geochim. Cosmochim. Acta* **2015**, *150*, 106−124.
(34) PNNL. eSTOMP User Guide. http://stomp.pnnl.gov/estomp_guide/eSTOMP_guide.stm (accessed February 15, 2017).
(35) DOE *Final Site Observational Work Plan for the UMTRA project Old Rifle site GJO-99-88-TAR*; DOE: Grand Junction, CO, 1999.
(36) Wang, Z.; Ulrich, K.-U.; Pan, C.; Giammar, D. E. Measurement and Modeling of U(IV) Adsorption to Metal Oxide Minerals. *Environ. Sci. Technol. Lett.* **2015**, *2* (8), 227−232.
(37) Abdelouas, A.; Lutze, W.; Nuttall, E. Chemical reactions of uranium in ground water at a mill tailings site. *J. Contam. Hydrol.* **1998**, *34* (4), 343−361.
(38) Beller, H. R. Anaerobic, nitrate-dependent oxidation of U(IV) oxide minerals by the chemolithoautotrophic bacterium Thiobacillus denitrificans. *Appl. Environ. Microbiol.* **2005**, *71* (4), 2170−2174.
(39) Beller, H. R.; Legler, T. C.; Bourguet, F.; Letain, T. E.; Kane, S. R.; Coleman, M. A. Identification of c-type cytochromes involved in anaerobic, bacterial U(IV) oxidation. *Biodegradation* **2009**, *20* (1), 45−53.
(40) Moon, H. S.; Komlos, J.; Jaffé, P. R. Biogenic U(IV) oxidation by dissolved oxygen and nitrate in sediment after prolonged U(VI)/Fe(III)/SO42- reduction. *J. Contam. Hydrol.* **2009**, *105* (1−2), 18−27.
(41) Yabusaki, S.; Şengör, S.; Fang, Y. A uranium bioremediation reactive transport benchmark. *Computat Geosci* **2015**, *19* (3), 551−567.
(42) Williams, K. H.; Wilkins, M. J.; N'Guessan, A. L.; Arey, B.; Dodova, E.; Dohnalkova, A.; Holmes, D. E.; Lovley, D. R.; Long, P. E. Field evidence of selenium bioreduction in a uranium contaminated aquifer. *Environ. Microbiol. Rep.* **2013**, *5*, 444−452.
(43) Yabusaki, S. B.; Fang, Y.; Williams, K. H.; Murray, C. J.; Ward, A. L.; Dayvault, R. D.; Waichler, S. R.; Newcomer, D. R.; Spane, F. A.; Long, P. E. Variably saturated flow and multicomponent biogeochemical reactive transport modeling of a uranium bioremediation field experiment. *J. Contam. Hydrol.* **2011**, *126* (3−4), 271−290.
(44) Yabusaki, S. B.; Fang, Y. L.; Waichler, S. R. Building conceptual models of field-scale uranium reactive transport in a dynamic vadose zone-aquifer-river system. *Water Resour. Res.* **2008**, *44* (12), 24.
(45) Qafoku, N. P.; Zachara, J. M.; Liu, C. X.; Gassman, P. L.; Qafoku, O. S.; Smith, S. C. Kinetic desorption and sorption of U(VI) during reactive transport in a contaminated Hanford sediment. *Environ. Sci. Technol.* **2005**, *39* (9), 3157−3165.
(46) Liu, C. X.; Zachara, J. M.; Qafoku, N. P.; Wang, Z. M. Scale-dependent desorption of uranium from contaminated subsurface sediments. *Water Resour. Res.* **2008**, *44* (8), 13.

DOI: 10.1021/acs.est.6b04873
Environ. Sci. Technol. 2017, 51, 3307−3317